

# Sensor fusion and correlation of X-ray tomography and XRF data for drill core analysis

Jonathan HANSEN<sup>1</sup>, Virginia VOLAND-SALAMON<sup>1</sup>, Tobias C. KAMPMANN<sup>2</sup>,  
Markus FIRSCHING<sup>1</sup>, Oleksiy SAMODVIGA<sup>1</sup>, Alexander ENNEN<sup>1</sup>,  
Norman UHLMANN<sup>1</sup>

<sup>1</sup> Fraunhofer Development Centre X-ray Technology EZRT, Fürth, Germany

<sup>2</sup> Department of Civil, Environmental and Natural Resources Engineering, Division of  
Geosciences, Luleå University of Technology, Luleå, Sweden

Contact e-mail: jonathan.hansen@iis.fraunhofer.de

**Abstract.** State of the art analysis techniques on drill cores for exploration purposes, including X-ray fluorescence (XRF), laser-induced breakdown spectroscopy (LIBS) or Raman spectroscopy are used to derive mineralogical information. Since this sensor data corresponds to materials that occur on the surface of the core, inclusions (e.g. diamonds) cannot be detected. In addition, information outside of the measurement position is not taken into account and may lead to misinterpretation or the miss of certain elements. X-ray computed tomography (CT) and radioscopy provide data about the entire sample as well as inlying structures based on X-ray absorption. As a drawback, CT is time-consuming and the material information is not explicit.

For the enhancement of geological interpretation, we propose to apply sensor data fusion techniques in order to unite both depth information as well as reliable material data information from surface measurement techniques. This leads to more substantial information of the drill core.

For further insights in the feasibility we investigate the correlation of XRF data at varying abstraction levels with CT data, i.e. grey value information.

The applied XRF technique involves the fact that the data is not acquired continuously but discrete point by point. This is accompanied by the circumstance that the spatial resolution of the acquired data has a different magnitude than the CT-data. Both facts result in the challenge to register the XRF data coming from a one-dimensional scan line with a micro-CT volume. The experiments must be planned in a way that location and orientation of the scan data are well-known and reproducible.

In the experiments, the acquired and registered data of a defined drill core is analysed with respect to correlation and fusion capability. The experimental setup will be presented and results will be discussed.

## 1 Introduction

Sensor based analysis of drill cores has been well established in mining and exploration activities in order to support geologists extracting valuable information from drill cores and samples. With huge amounts of cores coming from drilling activities, the need for automated inspection and computer aided analysis rises constantly. Different analysis techniques like LIBS, XRF or optical inspection are able to derive detailed and reliable information from the



core but are limited to analyse only the surface. In addition providing measurement data covering most of the surface is unpractical due to handling of the drill cores or samples. While most of the measurement techniques provide information based on a line or spot scan, the results from the surface must be extrapolated to the entire core.

In contrast, computed tomography (CT) measurements are able to provide information on the entire core but lack the possibility to deduce chemical or geological information in the same detail and precision.

In order to obtain precise mineralogical information as well as volumetric data considering the entire core, we propose a way of combining both measurement techniques with the aim of improving the overall available data of the core.

## 2 Experimental Method

### 2.1 Drill core samples and data generation

Two drill core samples of 12 cm and 16 cm length respectively, have been chosen in close collaboration with the Geological Survey of Finland (GTK) and its drill core archive. The samples have been characterized petrographically using standard optical methods, with special emphasis on the chosen locations for the analytical lines (see section 3). To follow the attempt of combining multiple measurement techniques we performed XRF and CT scans on the selected drill cores. The measured data was then superimposed and combined.

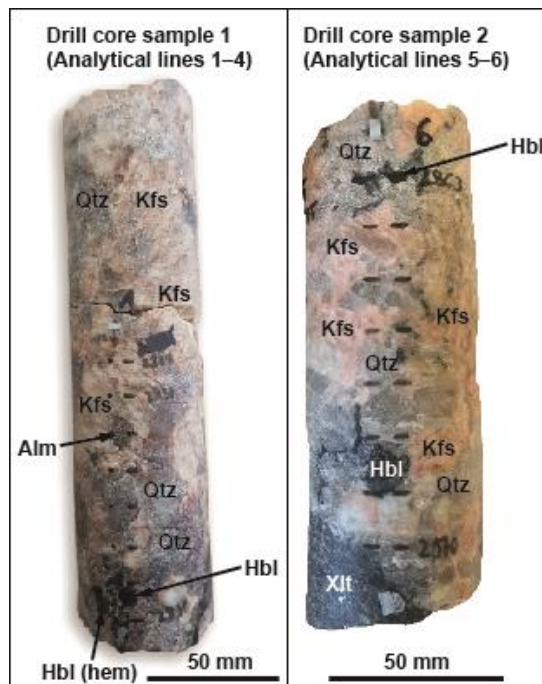


**Fig. 1.** Optical photographs of the studied drill core samples, including analytical lines 1 (drill core sample 1) and 6 (drill core sample 2). Macroscopically present minerals are marked according to the petrographic analysis. See Table 2 and text for more information. Abbreviations: Qtz = Quartz; Kfs = K-feldspar; Alm = Almandine garnet; Hbl = Hornblende; Hbl (hem) = Hornblende with hematite staining; Xlt = Xenolith fragment consisting of fine-grained biotite, hornblende and plagioclase.

#### 2.1.1 XRF

XRF-data were generated manually using a *Bruker S1 TITAN* series handheld XRF analyser. The locations on the surface of the core where chosen in a way that we defined six lines along

the core samples that looked promising in measuring all present minerals. This fostered differentiating between them in CT-analysis. Then, measurement sites were marked with a pen. The spots were placed in regular intervals of 10 mm (scans 1 and 2) or 20 mm (scans 3 and 4) respectively. The *SI TITAN* has an internal camera that was used to measure as close as possible around the predetermined spots.

Mineral distribution was ascertained using the *GeoChem* feature provided by *Bruker*.

### 2.1.2 CT

3D data was generated using a stop-and-go CT scan procedure that is common in diamond drill core scanning of samples similar to the ones used in this study. Scan parameters are listed in Table 1.

**Table 1.** Scan parameters as used for the CT-scans

Source-detector-distance (mm)	663.384	Tube voltage (kV)	220
Source-object distance (mm)	326.482	Tube current (mA)	0.18
Number of projections	1200	Exposure time (ms)	300
Voxel size ( $\mu\text{m}$ )	94.1765	Number of frames averaged	1

Apart from the raw data, the most important information to be used is the edge length of a single voxel within the 3D dataset. Based on this we can calculate the volume of a voxel cluster we estimate to be of a specific material.

### 2.1.3 Matching

Matching the data of different sources was possible by marking the XRF measurement segments with zinc plates, which are easily identifiable in the CT data due to their known shape and high absorption. Therefore, we were able to calculate the individual measurement locations in terms of 3D coordinates. Automation of this procedure is possible, due to the difference in signal of the zinc plates from the other present minerals in the samples. It may also be possible to superimpose the measurements utilising contained materials or minerals with significant signal in both techniques or simply by a known alignment of the sensors to each other within the measurement coordinate system.

## 2.2 Image Processing

The aim with the segmentation of the aforementioned areas is to determine the amount of Fe in the core samples. The segmentation process creates a mask that marks each voxel as either Fe or not. In future work, it should be investigated if a weighted mask is more suitable. Such mask would not only represent a binary decision (Fe: yes or no) but an approach closer to fuzzy logic.

There are two issues regarding the raw CT scan data:

1. Cupping: cupping artefacts are caused by beam hardening and lead to radial, non-equal grey value distributions in the core volume (Fig. 2). We managed to minimize the cupping effect by first calculating a median over the z-index of the whole core and then calculating a radial mean value over 100 angles.

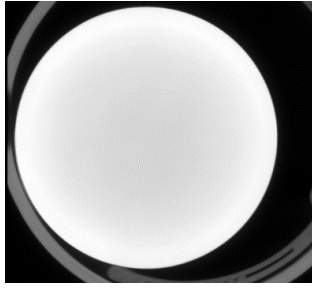


**Fig. 2.** Median of z-projection showing higher grey values on the border (lighter) than on the inside (darker).

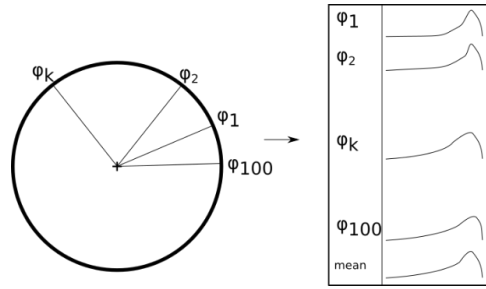


**Fig. 3.** Calculating a radial mean for multiple angles from the result of Fig. 2.

The averaged data was fitted via polynomial curve fitting to get a smooth curve (see Fig. 3). Based on the curve, the whole core volume data was corrected to achieve the same grey values for equal materials and densities in the core, independent of their distance to the core surface, which is crucial for approximating the total concentration of a certain material. In addition, the grey value outside the radius of the core was set to zero.

2. Noise: This is partly because of the acquisition method and partly due to the fact that minerals can be of a specific structure that may mimic a noise signal in 3D data. To eliminate most of the noise, we applied a specific type of median to the core volume data that would ignore values that are zero. This was necessary to ensure that the air around the core would not affect the calculated median value.

After these two problem solving steps, we noticed a better data quality (i.e. a more distinct grey value profile) by examining single slices of the 3D volume and individual plots. The denoising step was important to increase the overall contrast between different areas and lower the contrast within them, which was the starting point to begin segmentation.

### 2.3 Segmentation and Binarisation

For segmentation a k-means algorithm was applied. Alternative methods would include watershed segmentation and manual separation of histogram values. We settled with the k-means approach to be able to automate the process in the future. Some specific values for the algorithm were chosen manually: we set  $k=3$  to segment the data into background/air (low values), Si (mid values) and Fe (highest values). Manual starting points for the clustering were gathered by considering the volume histogram. We performed this step in order to ensure the reproducibility of the results.

We segmented solely for the grey-value of the CT scan and did not track any other features such as the size of specific connected clusters. After the segmentation we only kept the label representing Fe, the other voxels were set to zero. One main intention was to ensure the interpretability of the analysis results. The labelled volume contained clusters of different sizes, especially many small voxel clusters or even single voxels. The petrographic analysis suggested that the small clusters and single voxels do not correspond to Fe in reality. We hence deleted all clusters with sizes smaller than  $5\text{mm}^3$ . This threshold was selected arbitrarily according to the petrographic analysis and had minor impact on the analysis result itself.

### 3 Results

#### 3.1 Petrographic analysis

Both samples are gneisses with granitic to granodioritic composition and coarse grain sizes which in part resemble a pegmatitic texture. They belong to a suite of 1.8 – 1.9 Ga metamorphic granite gneisses representing a portion of the bedrock around Helsinki, Finland (Alan Butcher, personal communication 2019). Identified minerals in the samples include K-feldspar, quartz, plagioclase, hornblende (often hematite-stained) and almandine (Fe-rich) garnet. In core sample 2 (analytical lines 5 and 6), a xenolithic fragment occurs which consists mainly of fine-grained hornblende, biotite, quartz and plagioclase. This drill core sample generally contains lower amounts of quartz and higher portions of hornblende, probably representing a more intermediate composition compared with sample 1 (analytical lines 1–4). The encountered main minerals in the drill core samples, including their ideal chemical formulas, are summarized in Table 2.

**Table 2.** Main mineralogy of the drill core samples utilized in this study as identified in the petrographic analysis, including ideal chemical formulas. Chemical substitutions and trace elements can occur.

Mineral	Chemical formula
K-feldspar (orthoclase)	$\text{KAlSi}_3\text{O}_8$
Quartz	$\text{SiO}_2$
Plagioclase	$(\text{Na,Ca})(\text{Si,Al})_4\text{O}_8$
Hornblende	$(\text{K,Na})_{0-1}(\text{Ca,Na,Fe,Mg})_2(\text{Mg,Fe,Al})_5(\text{Al,Si})_8\text{O}_{22}(\text{OH})_2$
Hematite (present as staining on hornblende)	$\text{Fe}_2\text{O}_3$
Almandine garnet	$\text{Fe}_3\text{Al}_2(\text{SiO}_4)_3$
Biotite	$\text{K}(\text{Mg,Fe})_3\text{AlSi}_3\text{O}_{10}(\text{OH,F})_2$

#### 3.2 Matching

In general, grey values in a reconstructed CT-volume correspond to attenuation coefficients of the respective material: the higher the grey value, the higher the attenuation coefficient. In our case, the grey values are represented by arbitrary units. Correlation of the XRF- and CT-data sets provided the insight that high grey values (corresponding to the bright spots in the cross sections) show a correlation with the fraction of Fe compounds measured by the XRF scans. To provide this data, we listed the Al and Fe compounds, which represented the major share of minerals besides Si and plotted them onto an unwrapped view of the drill core surface provided by CT data (see Fig. 4). In order to analyse correlation, we created a line plot containing the Al- and Fe- fractions on the one hand and grey values on the other hand (Fig. 5). The impact of Fe on the grey values is clearly visible, while Al has minor impact.

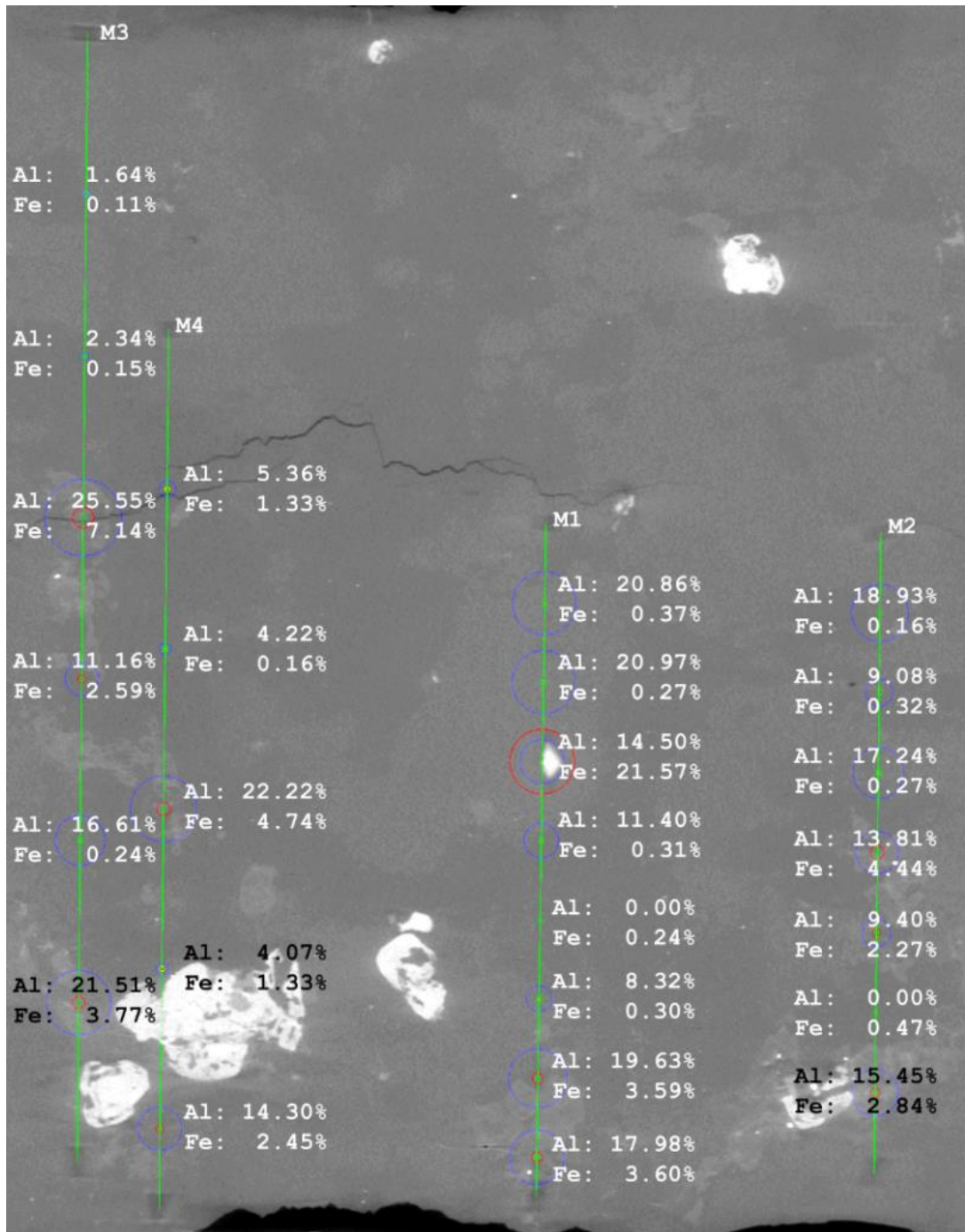


**Fig. 4.** Unwrapping of drill core surface.  
XRF Measurements marked in green, Fe marked by red circles, Al findings in blue.

Other minerals such as Al compounds could not be identified with good correlation in the CT data. This should be further investigated in using different approaches based on what features to correlate (not the grey values itself but the mean grey value in a defined area combined with the standard deviation in the region of interest for example). In order to be able to correlate more minerals in XRF and CT data, we need more drill cores and methods how to correlate the data.

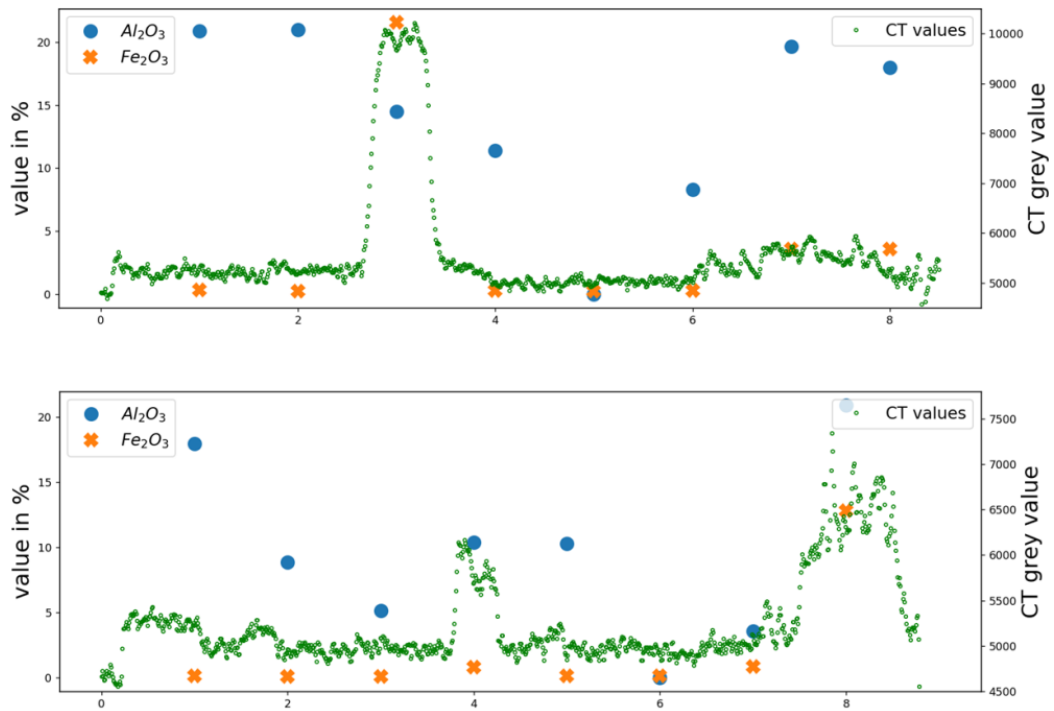


**Fig. 5.** Correlation between XRF data (blue o, orange x) and grey values from CT (green dots). It is clearly visible, that the occurrence of Fe leads to an increased grey value, while the occurrence of Al has comparably less impact.

### 3.3 Volume data and image processing

Following the workflow outlined above (see 2.2), we have a volume that contains binary information on whether the individual voxel in the original volume is to be taken as Fe or not. Calculating the number of voxels that were labelled to be Fe, we obtained the following data (Table 3):

**Table 3.** Combined results of the core analysis. The method allowed a determined fraction of Fe of 1.5 %, which correlates with the petrographic analysis.

	volume (cm <sup>3</sup> )	number of voxels	fractional part
drill core	204.48	244,806,465	100 %
Fe	3.07	3,673,824	1.50 %

The following images illustrate the steps applied to the volume. Every row shows one specific 2D slice from the same 3D volume in different stages of the processing.

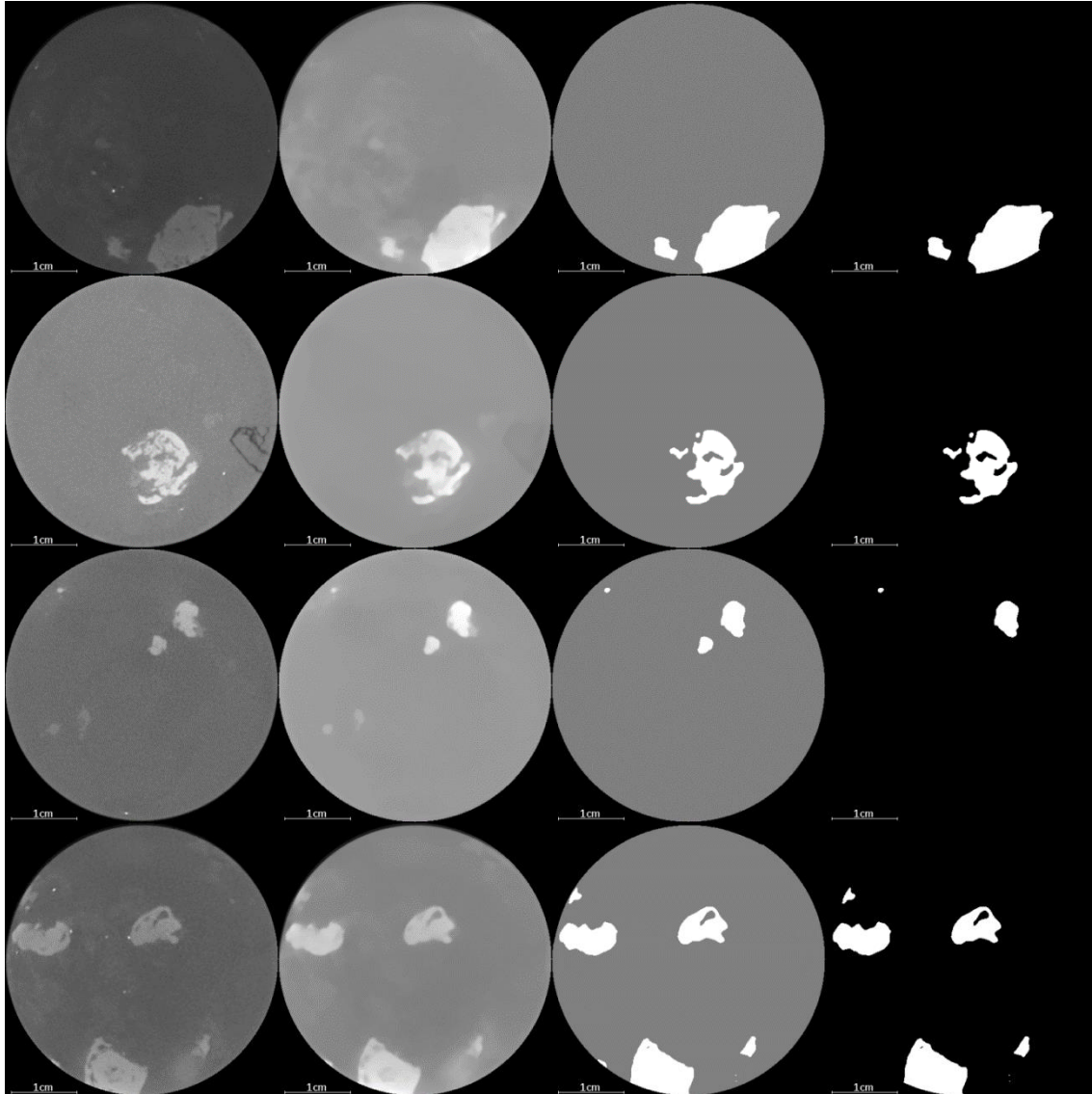


**Fig. 6.** Results at different stages of the workflow. The steps from left to right:  
 1: after having corrected the cupping artifact  
 2: after having applied denoising  
 3: after segmentation  
 4: after having eliminated small grains

The images show 2D cross-sections of a three-dimensional data set. All in step 4 eliminated areas belong to clusters of size smaller than  $5\text{mm}^3$ . All remaining single white pixels are directly connected to clusters larger than  $5\text{mm}^3$ . These clusters in general extend over several slices and may therefore appear smaller than they are.

All calculations were done using python with packages from *numpy*[2] and *scipy*[3] (*scipy.ndimage* in particular, [1]-[4]).

## 4 Conclusion and outlook

### 4.1 Performance of the developed methodology and possibilities for improvement.

The overall goal of extending the surface data into the 3D volume could be partially achieved. When working with the data we observed that handling the segmentation between Si and Fe was relatively stable while trying to separate Al or K from other materials did not work with the same reliability.

There is, of course, opportunity for improvements, especially when we consider investigating more samples. A few examples of improvements that will be worked on are:

- Extending the range of detectable materials by sharper CT-segmentation and gathering combinations of XRF-measurements and responding CT-information.
- Using the graphics card as a way to improve calculation speed.
- Automating the process of matching the coordinates of XRF- and CT-data by segmenting the CT data for markers.
- Finding an automatic way to provide parameters for the k-means algorithm.
- Identifying the radius and overall extent of the core in the 3D data automatically.

These steps should help to develop an algorithm that receives XRF- and CT-data as input, producing an estimate for Fe as an output. In regards to the precision of the proposed method, comparison to established surface technique based scanners as well as a direct chemical analysis is part of the ongoing work to validate the generated.

#### 4.2 *The significance of precise measurement of iron content in the context of geology and exploration*

The developed methodology has been demonstrated to accurately determine the presence and three-dimensional distribution of Fe in the processed drill core sample. Iron is present in the crystal lattice of nearly all minerals present in the studied core samples (Table 2), with the notable exception of quartz (pure SiO<sub>2</sub>). The minerals with the highest Fe content in these samples are expected to be almandine garnet (up to 33.66 wt% Fe), as well as hematite staining on hornblende (69.94 wt% Fe). The comparison between the petrographic analysis and the CT images of the cores leads to the interpretation that the brightest areas in the CT images represent almandine garnet. Hematite staining is also identifiable, but not as prominent which is probably due to its subordinate character (staining on hornblende).

The distribution of Fe in geological samples has important implications for exploration for metallic ore deposits. Alteration haloes of hydrothermal ore deposits, such as volcanogenic massive sulphide deposits, for example, typically experienced Fe enrichment to varying degrees during fluid flow and ore formation. This will lead to the formation of Fe-rich minerals such as chlorite and almandine garnet, the latter especially in metamorphosed deposits. Recent studies demonstrate that the three-dimensional distribution of Fe content in rocks surrounding hydrothermal ore deposits, based on both whole-rock geochemical data and mineral-chemical analysis, can be utilized to identify vectors towards mineralization ([5]). For this reason, methods that are able to accurately determine the distribution of Fe-rich minerals and general Fe content in rocks will aid geologists in the efficient targeting of ore deposits. In this context, we evaluate the herein developed method as a valuable contribution towards more objective and automatized processes in exploration, worthy of further investigation and development.

## 5 References

- [1] <https://www.python.org>
- [2] <http://www.numpy.org>
- [3] <https://www.scipy.org>
- [4] <https://docs.scipy.org/doc/scipy/reference/tutorial/ndimage.html>
- [5] Kampmann TC, Jansson NJ, Stephens MB, Majka J, Lasskogen J (2017) Systematics of Hydrothermal Alteration at the Falun Base Metal Sulfide Deposit and Implications for Ore Genesis and Exploration, Bergslagen Ore District, Fennoscandian Shield, Sweden. *Economic Geology* 112, 1111–1152.